Transmission through nonlinear barriers

Arthur R. McGurn*
Department of Physics, Western Michigan University, Kalamazoo, Michigan 49008-5252, USA
(Received 30 August 2007; revised manuscript received 11 December 2007; published 5 March 2008)

The transmission characteristics of simple nonlinear barriers are studied as functions of the nonlinearity of the barrier media. Two different types of nonlinear systems are considered. The first system is described by one-dimensional difference equations modeling a photonic crystal waveguide of linear optical media containing a barrier of Kerr nonlinear media. An initial treatment of this was given in Phys. Rev. B **69**, 235105 (2004). The second system is a time barrier described by the finite iteration of the logistic mapping. The conditions under which these systems exhibit transmission resonances are investigated. In the Kerr system, resonances are characterized by the excitation of intrinsic localized modes, discrete dark solitonlike excitations, and renormalized Fabry–Pérot excitations. In the logistic system, other types of modes are observed in connection with barrier resonances.

DOI: 10.1103/PhysRevB.77.115105 PACS number(s): 89.75.Kd, 05.45.−a, 42.65.Sf

I. INTRODUCTION

The study of patterns generated from nonlinear mappings has a long history.[1–7] A recent example is found in chaos associated with solutions of the logistic mapping and the various attractors characterizing these solutions.[1–3] From the simplest types of nonlinearity, the logistic mapping and its variant forms give complex patterns unlike those from linear mappings. Turing patterns in chemical and biological systems are additional examples of the generation of complex behaviors.[1,4–6] In this case, complexity is observed in the interplay of the rate of diffusion and reactive transitions for various inhomogeneous processes. In even simpler systems, Wolfram[7] has shown that a small set of short, compact, recursive rules can generate amazingly complex pattern behaviors. Here, complex behavior follows from a repetitive application of a simple rule. A common element of all these studies is that the introduction of nonlinearity to a system, even as a simple perturbation, often leads to fundamental changes in the dynamics. Consequently, systems that are relatively simple to understand in their linear limit exhibit an intricate complexity upon the introduction of nonlinearity.

In this paper, we look at another type of pattern formation, i.e., one found in finite nonlinear systems. In particular, the transmission coefficient of nonlinear barriers will be studied as a function of the barrier media, and the maxima of the transmission coefficient (i.e., the resonant transmission peaks) will be located in the space of parameters characterizing the nonlinearity of the barrier media. In the limit of the linear media barrier, the transmission behaviors are quite simple, but upon the introduction of nonlinearity and with increasing nonlinearity, the plot of the transmission peaks in the parameter space of the nonlinear media becomes increasingly complex. The object of the study will be to understand how the topographical features in the plot of the transmission peaks in the parameter space of the nonlinear media are associated with the resonantly excited modes in the nonlinear barrier media. Two different types of systems will be treated and compared. The first system is a barrier of Kerr nonlinear media in a photonic crystal waveguide of linear dielectric media.[8–13] The transmission of waveguide modes through the barrier will be obtained in terms of the two parameters characterizing the Kerr dielectric medium.[8] This type of system has been the focus of much recent work on possible electro-optical device applications.[8–10] In this regard, the interest is in short barriers which can be easily fabricated for applications, e.g., a barrier of five Kerr sites can support solitonlike modes that can be of interest in switching applications or in the generation of large fields within the barrier media.[8,10] As we shall see, these types of barriers exhibit complex behaviors which need to be understood when the conditions for generating particular types of barrier modes are required. (As for modeling nonlinear barriers in general, it may be interesting to note that under certain restricts on its parameters, the photonic waveguide equations can describe a chain of harmonically coupled atoms containing a barrier of anharmonically coupled atoms.[13]) The second system is a barrier formed from the finite application of the logistic mapping.[1–3] The logistic mapping is a famous example of a simple nonlinear model (often used in population studies) which tends to generate surprisingly complex patterns in its solutions and is a natural choice for making a system in which to study the effects of nonlinearity. This system has a different type of nonlinearity than that of the photonic crystal application, but the patterns formed in its finite barrier transmission problem can be understood in many of the same ways as those of the photonic crystal barrier system. Specifically, the nonlinearity of the system can be characterized in terms of two parameters. If one defines a resonant transmission of the population density as the unchanging transmission of the population density through the barrier (similar to maximally efficient resonant transmission through the photonic crystal barrier), a transmission map in the parameter space of the barrier can be made that is similar to that of the photonic crystal problem and a similar association of barrier wave functions with topographical features in the transmission map is also found. Both systems exhibit different types of nonlinearity, but will be seen to exhibit many qualitatively similar properties of resonant transmission and of the resonantly excited wave functions found in the different barrier materials.

In the study of the transmission of light through a Kerr nonlinear barrier in a photonic crystal waveguide, we investigate the pattern of resonant transmissions generated in the

parameter space characterizing the nonlinearity of the system.[8–10] The recursion relation considered was obtained in Refs. 11–13, where some of the properties of the system it describes were originally studied. The system is based on a two-dimensional photonic crystal consisting of infinite parallel axis dielectric cylinders arranged on a square lattice.[14–17] This gives an electromagnetic band structure for modes moving in the plane of the lattice with a series of stop and pass bands. A waveguide is formed in the photonic crystal by replacing a row of cylinders by cylinders with different dielectric properties so that guided modes at stop band frequencies propagate in the plane of the lattice along the waveguide cylinders.[7–12,15–21] The waveguide treated is infinitely long and straight and contains a barrier consisting of a finite number of replacement cylinders with Kerr nonlinear dielectric media. (Here, the only nonlinearity is in the barrier materials.) The transmission of a guided mode incident on the barrier is computed in terms of the barrier nonlinearity.[8–10,13,14,22–25]

Starting from the limit of a barrier of linear dielectric media, the transmission is computed for increasing nonlinearity. The object is to study the peaks in the transmission coefficient, to find their origins, to classify the patterns that arise in the peak distributions when presented as functions of the parameters describing the Kerr nonlinear media, and to associate these patterns with various resonantly excited modes of the barrier media. It is found that the patterns of transmission peaks distributed over the parameter space describing the nonlinearity exhibit a complexity that is explained in terms of the existence of intrinsic localized modes,[10,13,20,21,25–28] dark solitonlike discrete modes,[13,25,29–33] renormalized Fabry–Pérot modes, and other more complex barrier modes. Depending on the boundary conditions of the waveguide modes at the barrier edges, the excitations in the barrier can, in some instances, be found to shift position within the barrier media.

For comparison, results are also presented for studies of the logistic mapping. Here, a finite time barrier is treated in which the mapping is iterated for a fixed finite number of time steps, and resonant transmission is defined as the case in which the input at the initial barrier time is equal to the output at the final barrier time. The system is restricted to be conservative in this sense. The resonant transmission is studied in the parameter space of the nonlinearity, and similar patterns and behaviors to those found in the waveguide problem are observed. In some instances, though, the nature of the barrier excitations associated with the resonant transmissions are different, but excitations reminiscent of intrinsic localized modes, dark solitonlike modes, and Fabry–Pérot like resonances are observed along with the shifting of these modes within the barrier with changing boundary conditions.

In Sec. II, a brief review of the difference equations for the waveguide is given, the transmission resonances are presented in the parameter space of the nonlinearity, and the patterns in this plot are explained. In Sec. III, a brief discussion is made of the logistic mapping model and results are presented for the transmission resonances in the parameter space of its nonlinearity. In Sec. IV, conclusions are presented.

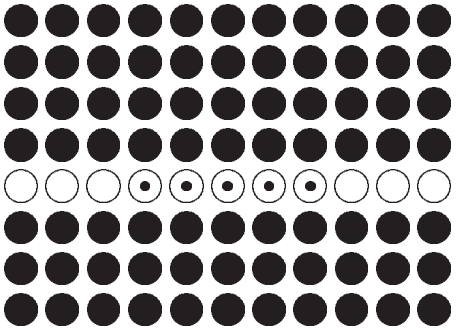

FIG. 1. Schematic drawing of the waveguide and the waveguide barrier of Kerr nonlinear media represented in the x-y plane. The dark circles are the cylinders of the photonic crystal, the open circles are the cylinders of the waveguide of linear media, and the open circles containing a dot are the cylinders of the barrier. The cylinders are perpendicular to the x-y plane.

II. WAVEGUIDE TRANSMISSION MODEL

The transmission through a finite barrier of Kerr nonlinear replacement cylinders embedded in a photonic crystal waveguide of linear dielectric media is treated. The model considered was originally discussed in Ref. 8 for a barrier of five cylinders containing Kerr media, and its properties were obtained from solutions of a set of difference equations. In the model, the replacement cylinders forming the waveguide and barrier differ from the cylinders of the bulk photonic crystal only by the addition of a small amount of dielectric material about the axis of each cylinder so that the electric field of the guided modes is separately constant over the added material in each replacement cylinder. The difference equations relate the fields at the centers of the replacement cylinder axes to one another. For a detailed discussion of the origin of the difference equations, the reader is referred to Refs. 11–13 and a brief summary of the discussions is also found in Appendix A.

The interest in the barrier model of five Kerr sites is twofold. From a theoretical standpoint, it was shown in Ref. 8 that this is the smallest barrier array in which intrinsic localized modes can be generated and identified. These types of modes have possible electro-optics applications.[20,21] From the standpoint of technological interest, small barriers are the easiest to make and implement in applications.[20,21] It is, consequently, useful to understand the behaviors of small systems over a large range of nonlinearities in order to judge the requisites for their applications. As will be seen in the paper, a wide variety of intricate and interesting behaviors are found in the small barrier limit, and it is best to start with a classification of these.

A. Review of model equations

The waveguide channel and the barrier of five consecutive waveguide channel sites are along the x axis of a square lattice photonic crystal.[8] Figure 1 gives a schematic representation of the system. The photonic crystal outside the waveguide and barrier is represented in Fig. 1 by dark circles. The five barrier sites, containing Kerr nonlinear me-

dia, are shown as five open circles with center dots and the waveguide sites composed of linear media are open circles. The barrier sites are labeled in the lattice by $(n,0)$ for $-2 \leqslant n \leqslant 2$, and the linear media waveguide sites are labeled by $(n,0)$ for $n<-2$ or $n>2$. The difference equations of the system for the electric field polarized parallel to the cylinder axes are[8]

$$E_{n,0} = f(n,E_{n,0})E_{n,0} + b[f(n+1,E_{n+1,0})E_{n+1,0} + f(n-1,E_{n-1,0})E_{n-1,0}], \quad (1)$$

where

$$f(n,E_{n,0}) = \begin{cases} g_l, & n>2 \\ g[1+\lambda|E_{n,0}|^2], & -2 \leqslant n \leqslant 2 \\ g_l, & n<-2. \end{cases} \quad (2)$$

Here, $E_{m,j}$ is the electric field at the (m,j) lattice site, g_l characterizes the properties of the dielectric cylinders in the linear media waveguide, and g and the Kerr parameter[22,23] $\lambda \neq 0$ characterize the properties of the dielectric cylinders in the barrier of Kerr media. (See Appendix A for further details about the parametrization.)

A solution of Eqs. (1) and (2) for electromagnetic waves incident on the barrier from the left is of the general form

$$E_{n,0} = ue^{ikn} + ve^{-ikn} \quad (3)$$

for $n<-2$,

$$E_{n,0} = txe^{ikn} \quad (4)$$

for $n>2$ with t and x real, and

$$E_{n,0} = a_n e^{i\theta_n} \quad (5)$$

for $-2 \leqslant n \leqslant 2$. Substituting into Eqs. (1) and (2) allows for the solution of the transmission coefficient, $T=|tx/u|^2$, as a function of g and t for fixed λx^2. [Note that the transmission coefficient of the nonlinear system only depends on the nonlinearity characterized by the Kerr parameter,[22–24] λ, and transmitted wave amplitude, xt, through the dimensionless combination $\lambda(tx)^2=(\lambda x^2)t^2$. The transmission coefficient obeys a type of law of corresponding states, in which a fixed value of $\lambda(xt)^2$ can represent many systems with different values of λ and different values of xt]. By choosing λx^2 to be a fixed dimensionless parameter, t is a dimensionless parameter which adjusts the strength of the nonlinearity.

The discussions later are made for parameters used in Ref. 8. Of these parameters, those of the bulk photonic crystal are from an earlier experimental study on photonic crystals.[34] The parameters have been used in many studies[8,9,11–13,20,21] and can be considered as typical of photonic crystal systems, giving a band structure of the type commonly found in many photonic crystal systems and waveguide dispersion relations of a type found in many studies of photonic crystals.[15–20] Specifically, in the presentation later, we use the parametrization $b=0.0869$, $\lambda x^2=0.005$, and $k=3.0$, and the dispersion relation of the modes in the linear media waveguide (which relates the value of g_l needed to support a mode with the phase, k, along the waveguide) is given by Ref. 8 as $g_l = 1/[1+2b\cos(k)]$. In Appendix A, general expressions for these parameters in terms of the properties of the photonic crystal are given along with an outline of their origins. More detailed discussions are available in the literature in Refs. 11–13. Since the photonic crystal is an artificial device, its properties can be tailormade to fit many specifications, either by changing its dielectric properties or the sizes of its components. In particular, in Ref. 10 we have presented discussions on how the b couplings of our theory can be adjusted by changing the separation of the waveguide channel sites so that nearest-neighbor coupling theories apply. This is generally due to the fact that the waveguide modes occur at stop band frequencies, which results in a rapid decay of excitations that are injected into the system at stop band frequencies. Consequently, the nearest-neighbor couplings can be relatively small.

B. Transmission in the parameter space of the nonlinear media

Barrier transmission is studied as a function of the parameters characterizing the nonlinearity of the barrier material. Specifically, the transmission coefficient is characterized by a series of peaks or maxima in the two-dimensional parameter plane defined by the variables g and t, where $t=0$ for a barrier of linear media, and as t increases, the nonlinearity of the barrier media increases. The topography of peaks in the (t,g) plane is determined, and various groupings of peaks are correlated with different types of excited barrier modes.

Figure 2 presents the plots of the transmission peaks in (t,g) space. Figure 2(a) shows the positions of all peaks having transmission coefficient maxima, T, in the range $0.0 \leqslant T \leqslant 1.0$. The remaining subfigures present a break up of the distribution of peaks so that in Fig. 2(b) are peaks with $0.75 \leqslant T \leqslant 1.0$, in Fig. 2(c) are peaks with $0.50 \leqslant T \leqslant 0.75$, in Fig. 2(d) are peaks with $0.25 \leqslant T \leqslant 0.50$, and in Fig. 2(e) are peaks with $0.10 \leqslant T \leqslant 0.25$. In Fig. 2(b), some peaks have been singled out to be the focus of later discussions. All plots are made by computing the transmission coefficient as a function of g for each t and by locating the peaks, which are then presented in Fig. 2. It is seen that the peaks are arrayed into a number of different groupings in the (t,g) plane, and most of the significant transmission peaks occur for $g \geqslant 0.5$. The bulk of the latter considerations will be on the topography in Fig. 2(b) for $0.75 \leqslant T \leqslant 1.0$.

To understand the transmission patterns, the barrier wave functions associated with different groupings of transmission peaks in the (t,g) plane are examined. Figure 3 presents a number of plots for the barrier wave functions at different (t,g). The modes of the nonlinear media are displayed in plots of $\lambda|E_{n,0}|^2$ versus $n=-2$, -1, 0, 1, and 2, while results for linear media barriers are given in plots of $|E_{n,0}|^2$ versus n. We now discuss these plots.

Results for the $t=0$ (linear barrier media) limit are shown in Fig. 3(a). The guided modes excite five different Fabry–Pérot modes. These are at $(t,g)=(0.0,0.8767)$, (0.0,0.9490), (0.0,1.0568), (0.0,1.1636), and (0.0,1.2078). In the plot, the maximum mode amplitudes are arbitrary because the dynamics of the linear media solutions do not depend on the mode amplitude. As t increases, the system becomes nonlinear and

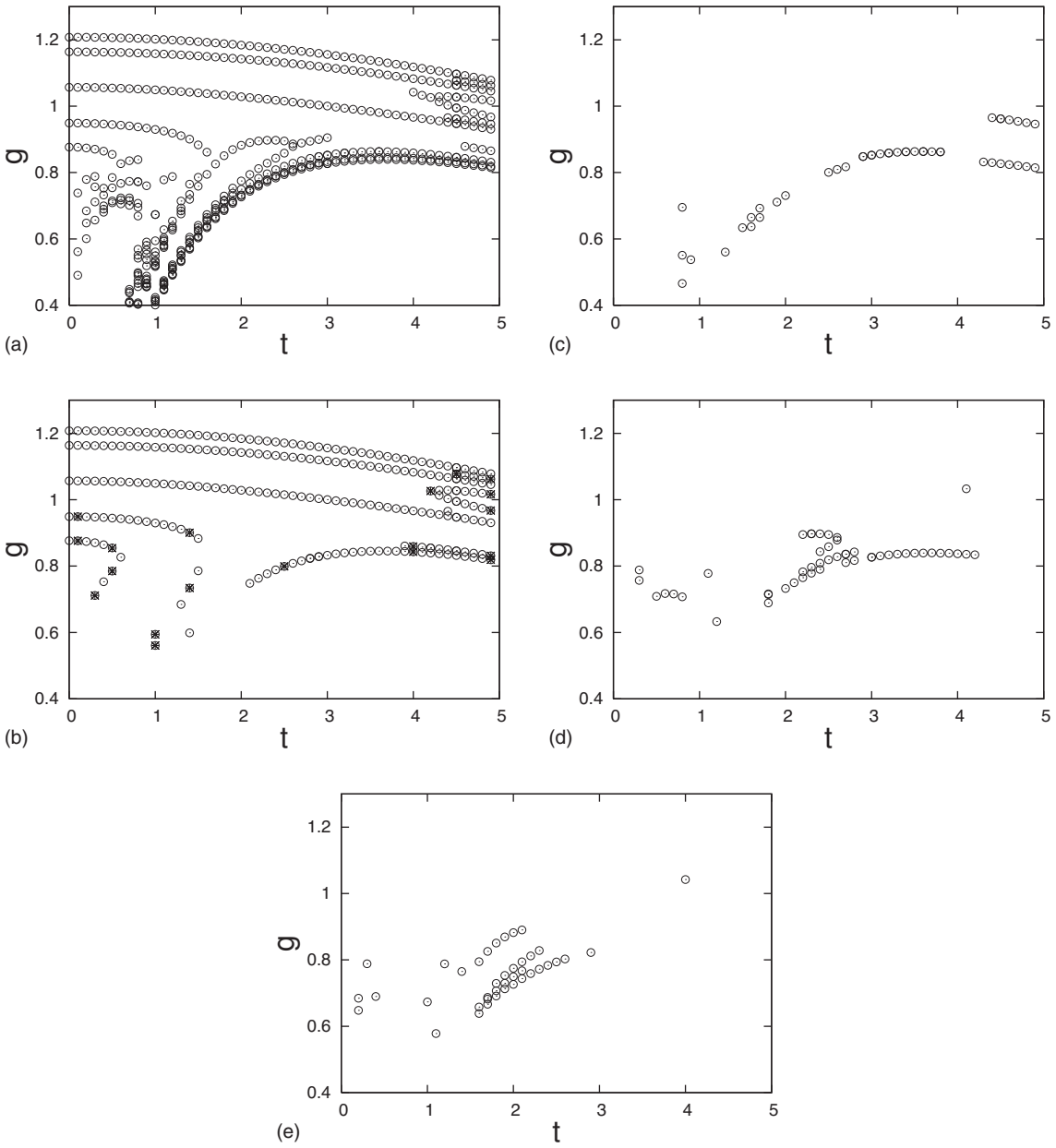

FIG. 2. Positions of the peaks of the transmission coefficient for a barrier of five sites in the (t,g) plane presented for (a) $0.0 \leqslant T \leqslant 1.0$, (b) $0.75 \leqslant T \leqslant 1.0$, (c) $0.5 \leqslant T \leqslant 0.75$, (d) $0.25 \leqslant T \leqslant 0.5$, and (e) $0.1 \leqslant T \leqslant 0.25$. Some peaks have been singled out in (b) for discussions in the text.

the modes that evolve from (0.0,1.0568), (0.0,1.1636), and (0.0,1.2078) give the three top curves in Fig. 2(b) for $0.0 \leqslant t \leqslant 4.0$. The nature of $\lambda|E|^2$ as a function of site position in the barrier for the excitations along these curves is found in each case to be similar to that in the corresponding linear modes. The amplitudes of the modes, however, are set by the nonlinearity and increase with increasing nonlinearity. This is also found to be the case for $0.0 \leqslant t \leqslant 1.4$ for modes that evolve from the mode at (0.0,0.9490). These modes all have similar features to the linear barrier mode, but have renormalized amplitudes.

A group of modes associated with the (0.0,0.8767) linear mode for $0.0 < t \leqslant 0.5$ will now be discussed. Specifically, results for (0.1,0.8761)and (0.5,0.8549) are presented in Fig. 3(b). The modes of this branch exhibit a mild peak which increases with increasing nonlinearity. Eventually, the branch makes a connection with a branch of intrinsic localized modes originating at (0.3,0.7114) and rising to meet it at (0.6,0.8269). The wave functions of the intrinsic localized modes at (0.3,0.7114) and (0.5,0.7849) are shown in Fig. 3(b). They exhibit more pronounced peaks than do the modes in the branch arising from the (0.0,0.8767) mode, and this is evidence of the importance of nonlinear effects of their origin. Further association of these modes with the resonant excitation of intrinsic localized modes are made, as in Ref. 8, by comparing their wave functions with those of intrinsic localized modes in an infinite Kerr barrier. The theory in Ref. 13 for the infinite Kerr barrier is used to make this compari-

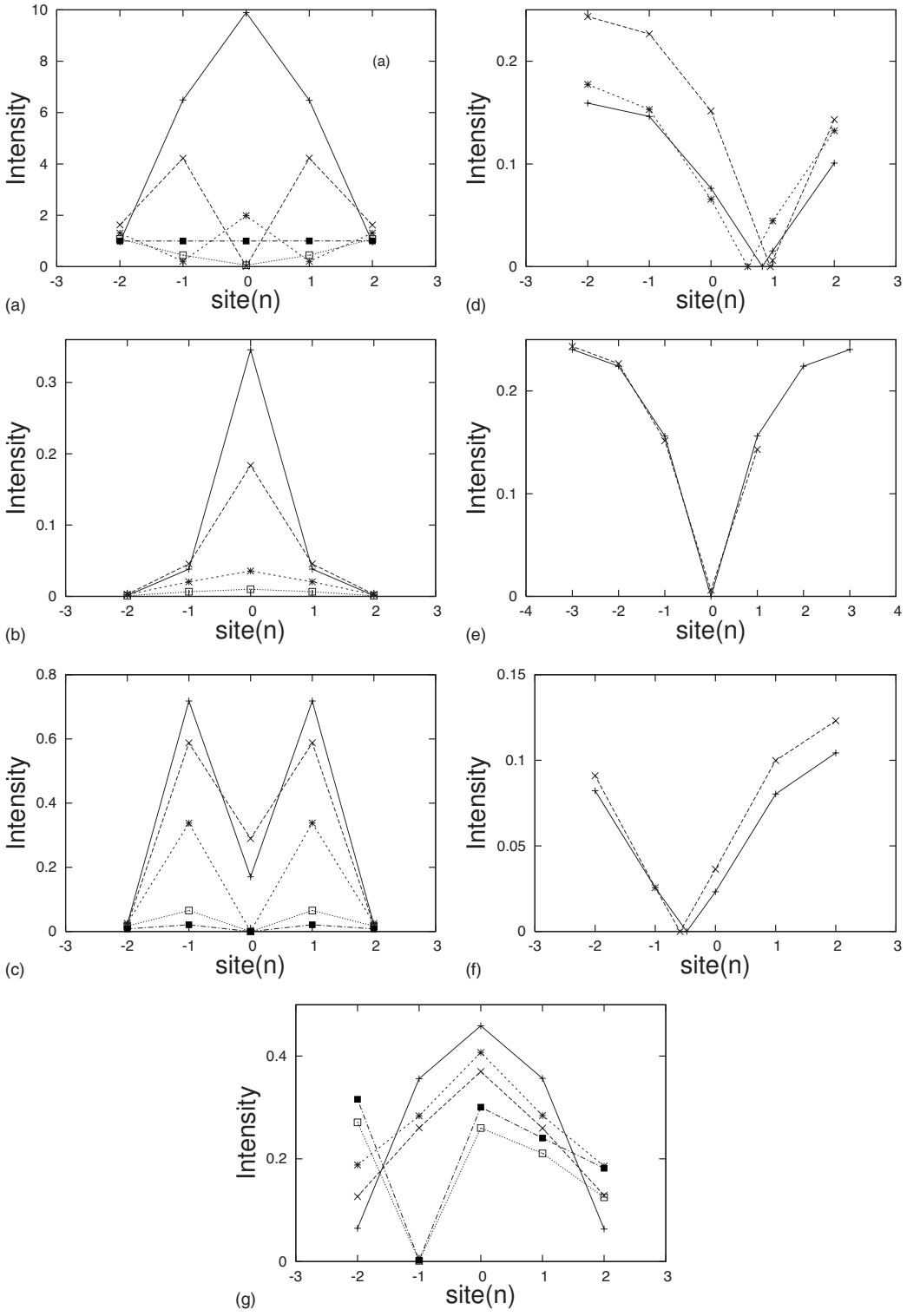

FIG. 3. Plot of field intensities at sites in the barrier. In (a), a plot of $|E_{n,0}|^2$ versus n in the $\lambda=0$ (linear limit) barrier is given for the Fabry–Pérot modes excited by the waveguide modes. (Note: $|E_{n,0}|^2$ is arbitrarily normalized in the case of the linear modes as the shape of the mode is the only interest here.) Results are shown for (0.0,0.8767), (0.0,0.9490), (0.0,1.2078), (0.0,1.1636), and (0.0,1.0568) from top to bottom at $n=1$. The remaining plots are for $\lambda|E_{n,0}|^2$ versus n for Kerr nonlinear barriers with modes at (b) (0.3,0.7114), (0.5,0.7849), (0.5,0.8549), and (0.1,0.8761) from top to bottom at $n=0$; (c) (1.0,0.5607), (1.0,0.5943), (1.4,0.7341), (1.4,0.9005), and (0.1,0.9489) from top to bottom at $n=1$; (d) (4.9,0.9676), (4.9,1.0162), and (4.2,1.0261) from top to bottom at $n=-2$; (e) (4.9,0.9676) (lower curve) compared with the dark solitonlike mode at $g=0.9722$ (upper curve); (f) (4.9,1.0622) and (4.5,1.0775) from top to bottom at $n=2$; and (g) (2.5,0.7991), (4.9,0.8190), (4.0,0.8428), (4.9,0.8312), and (4.0,0.8591) from top to bottom at $n=0$. In Fig. 2(b), the peaks entering into the discussions of the wave functions in Fig. 3 have been highlighted.

son. In this manner, the barrier mode at (0.3,0.7114) is associated with an intrinsic localized mode that exists in the infinite barrier limit for $g=0.7109$ with amplitudes of $\lambda|E_{0,0}|^2=0.346$, $\lambda|E_{\pm 1,0}|^2=0.0391$, etc., and the barrier mode at (0.5,0.7849) is associated with an intrinsic localized mode that exists in the infinite barrier limit for $g=0.7825$ with amplitudes of $\lambda|E_{0,0}|^2=0.183$, $\lambda|E_{\pm 1,0}|^2=0.0495$, etc. These values are in good agreement with the barrier results presented in Fig. 3(b). As a final point, it is also important to note that the branch of intrinsic localized modes ends before $t=0$ is reached, i.e., the intrinsic localized modes have no counterparts in the linear media barrier modes.

With increasing t, a second branch of modes is observed in Fig. 2(b) between $1.0 \leqslant t \leqslant 1.4$ for $0.50 \leqslant g \leqslant 0.95$ and appears to connect with the branch between $0.0 \leqslant t \leqslant 1.4$ that evolves from the linear mode at (0.0,0.9490). This second branch is interpreted as a case in which two intrinsic localized modes have been squeezed into the barrier. In Fig. 3(c), results are shown for the intrinsic localized pairs at (1.0,0.5607), (1.0,0.5943), and (1.4,0.7341). For comparison, results are also presented for modes at (0.1,0.9489) and (1.4,0.9005). These last two modes have much less amplitudes than those from the intrinsic localized modes so that their wave functions are not the result of the nonlinearity of the system. Again the branch of intrinsic localized modes disappears before the $t=0$ axis is reached.

Continuing these discussions to cases of increasing nonlinearities, consider features for $t \geqslant 4.0$ that occur between the top three branches spanning $0.0 \leqslant t \leqslant 5.0$ in Fig. 2(b). These features are suggestive of those associated with kink or so-called dark solitonlike modes.[28–33] In Fig. 3(d), results are shown for transmission peaks at (4.2,1.0261), (4.9,0.9676), and (4.9,1.0162) exhibiting intensity minima similar to those of dark solitonlike modes. In making the plots, the fields are computed at the integer labeled sites, and the minima observed between the $n=0$ and $n=1$ sites have been determined by linear interpolations. Here, the boundary conditions at the edges of the Kerr barrier gradually shift the position of the minima. Specifically, at the edges of the finite barrier, the conditions present in the infinite waveguide of Kerr media are only approximately met so the system resonates with the mode from the infinite system. A similar effect is found in the Stark effect, where the application of an external electric field changes the boundary conditions of the atomic electrons and results in a slight change in the electronic energy levels and a shift of the electronic probability distributions in space. Nevertheless, in the Stark effect, the perturbed electron states can still be seen to arise from their associated electronic states in the absence of an external electric field. In all the cases, the barrier has a tendency to resonate for the correct field intensities of the dark solitonlike mode and develop an associated resonant transmission. (This type of shifting of the wave functions with small changes in the boundary conditions at the barrier edges will also be seen later in the discussions of the modes of the logistic model.) In Fig. 3(e), a comparison is made of the dark soliton mode in an infinite barrier evaluated for $g=0.9722$, with the mode excited in the five site barrier at (4.9,0.9676). In the figure, the sites have been relabeled so that $n=0$ is near the minima, and the infinite barrier mode is obtained from the theory in Ref. 13. In Appendix B, a brief summary is given of the equations for the dark soliton mode discussed in Ref. 13 as these were removed from those original discussions. In addition, Appendix B gives an example of how boundary conditions can shift the minima of the dark solitonlike modes in the infinite barrier limit. The agreement in dielectric conditions and wave function intensities between the finite and infinite barrier results is good. Figure 3(f) shows results for modes at (4.5,1.0775) and (4.9,1.0622), which again agree with dark soliton results from the infinite barrier limit. It is important to note that the comparison here, however, with the infinite barrier results is made only because the wave functions and dielectric conditions under which the resonance in the finite barrier and the mode in the infinite barrier exist are very similar. It is suggestive that understanding the resonance may help understand the infinite barrier solution, and conversely. In addition, it is emphasized that the barrier of five sites is the smallest barrier that can contain the width of the resonant mode that simulates the dark solitonlike solution, and that a meaningful identification of such modes in smaller barriers is not possible. Such modes also do not evolve from modes found in smaller barriers. Similar to the case of intrinsic localized modes, the requirement for seeing dark solitonlike modes is that the width of the barrier is long enough to contain the peak or dip of either mode, respectively, and that the boundary conditions of the linear media waveguide modes at the edges of the finite barrier give a reasonable approximation of those at the corresponding positions of the mode in the infinite barrier. As seen from Fig. 2(b), these conditions are not easily met in the waveguide with barrier system.

Lower g from the kink modes are another set of features containing the representative modes at (2.5,0.7991), (4.0,0.8428), and (4.9,0.8190). The wave functions of these modes are shown in Fig. 3(g). They have rather broad peaks compared with the intrinsic localized modes discussed earlier. In addition, the nearest-neighbor sites to the peaks have much greater field intensities than those associated with intrinsic localized modes. The fields as a whole are also much greater that the intrinsic localized modes. These may find their origins in broad pulses found in the infinite barrier limit. Results are also shown for (4.0,0.8591) and (4.9,0.8312). These modes exhibit both peaks and minima and may arise from the heavy influence of the barrier boundary conditions on modes that are distorted from broader peaked modes found in the infinite barrier limit.

III. LOGISTIC MAPPING

Similar types of patternings in the parameter space of the nonlinearity and in the wave functions can be found from the logistic mapping.[1–5] The problem, though different than the waveguide problem, exhibits many similarities to it in the qualitative features of its solutions. The logistic mapping describes nonlinear changes in population densities with time. A barrier can be thought of as an interval of a fixed finite length of time, and the change in population density is a type of transmission of the population from the beginning to the

end of the time interval so that during this interval the population density increases, decreases, or remains the same. In the waveguide problem, we were interested in resonant transmissions in which most of the incident electromagnetic energy passed through a small barrier by resonant excitation of modes in the barrier. Let us extend this analogy to the logistic mapping and ask for the conditions that the initial population density passes unchanged through a small time barrier. We shall see that a similar pattern is generated in the parameter space of the nonlinearity of the logistic equation as that in the pattern space of the waveguide problem. In addition, modes similar to intrinsic localized modes and to dark solitonlike modes are found in regions of the logistic equation parameter space that are qualitatively similar to the regions of the parameter space of the waveguide problem in which intrinsic localized modes and dark solitonlike modes are found. This suggests that a general way of classifying the dynamical behavior of small nonlinear systems is by determining their resonant transmission properties for modes incident on them from the outside world as functions of the parameters characterizing the nonlinearity in the system. Excitations with similar types of wave functions cluster together in ridges found in the plot of the transmission coefficient in terms of the parameters characterizing the nonlinearity. Additional studies of the transmission characteristics of junctions formed from Kerr nonlinear dielectric media between several waveguides of linear dielectric media and from branching systems based on the logistic equation support these conclusions.[35]

Consider the problem of a finite iteration of the mapping (e.g., six iterations) and define a transmission resonance as the case in which the output at the final iteration is equal to the input into the first iteration. Adopting a similar notation to that used above, the logistic mapping is written as

$$t_{n+1} = g t_n [1 - t_n] \tag{6}$$

for $n=0-5$, and the wave function is defined as $\{t_n\}$ for $n=0-6$.

In Fig. 4(a), the transmission resonances are shown in the (t,g) plane for $0.0<t<1.0$ and $1.0\leqslant g\leqslant 4.0$, where t is the value of the initial input and final output. As in Fig. 2, the peaks cluster into a series of ridges, and the wave functions at different points in the same ridge exhibit closely related geometries. As an example of this, consider Fig. 4(b) which shows the extreme upper left hand corner of the (t,g) mapping. The four ridges shown exhibit four distinct wave functions, the examples of which are shown in Figs. 5(a) and 5(b). The excitations in Fig. 5(a) are reminiscent of intrinsic localized pulses in which a small input and output (for which the system has a small nonlinearity) result at an intermediate iteration in a highly nonlinear behavior in the vicinity of a peak. As in the case of the barrier problem, a sensitivity to the boundary conditions at the edges of the barrier is seen. Specifically, slight changes in the barrier conditions are seen to shift the peak, labeled (i), (ii), and (ii) in Fig. 5(a). In addition, the excitation observed in Fig. 5(b) appears as a superposition of two single peaked modes. This type of behavior was also observed in the excitations of the waveguide barriers in Fig. 3(c). At the extreme upper right hand corner

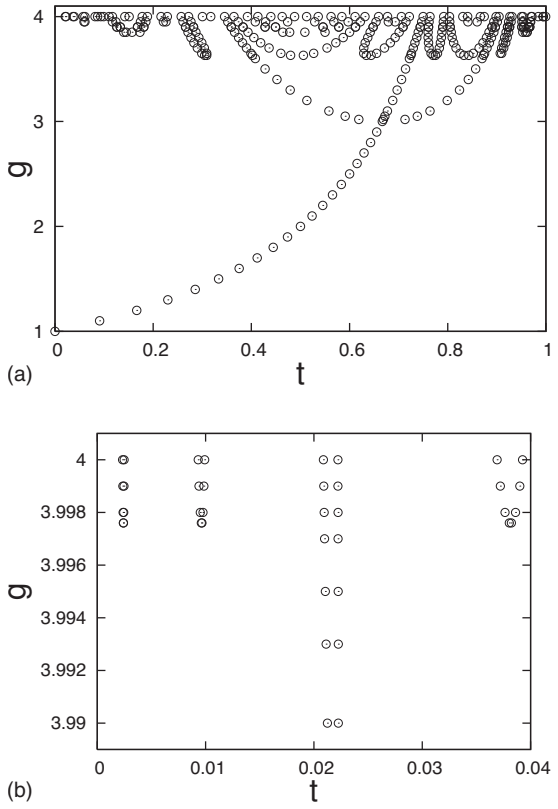

FIG. 4. Plot in the (t,g) plane of the contours of output equal to the original input. Six iterations of the logistic mapping are considered. In (a), the region of $0.0\leqslant t\leqslant 1.0$ and $1.0\leqslant g\leqslant 4.0$ is presented. In (b), the region of $0.0\leqslant t\leqslant 0.04$ and $3.988\leqslant g\leqslant 4.0$ of the far upper left hand corner of (a) is shown. The plots are obtained from a discrete set of runs.

of the (t,g) mapping, on the other hand, we see totally different types of wave functions compared to those in Figs. 5(a) and 5(b) in the two examples given in Fig. 5(c). For (0.999415,4.0) at the most extreme right, the form is reminiscent of a dark solitonlike pulse. Here, from an extremely large population density, a rapid minimum is found that eventually reverts to the original maxima. This behavior is, however, changed in the wave function of the next closest fixed point solution found at (0.994755,4.0). These types of behaviors are probably typical to a wide variety of iterative mapping for finite iterations. Outside couplings to the system that have small amplitudes, under the right conditions, can produce large peaks in the nonlinear media, and outside coupling to the system that have large amplitudes can, under proper conditions, produce drastic dips in the nonlinear media.

Another interesting behavior is found in the ridge of solutions forming a minimum in g as a function of t for the regions $0.4<t<0.9$ and $3<g<4$. These solutions exhibit wave functions that oscillate alternately from site to site within the barrier between a minimum and a maximum value and are reminiscent of the Fabry–Pérot modes found in Fig. 3(a). The phase of the oscillation shifts, however, as the line of states in the ridge arising from (0,1) is crossed. [Note: The modes in the line of states arising from (0,1) are modes of

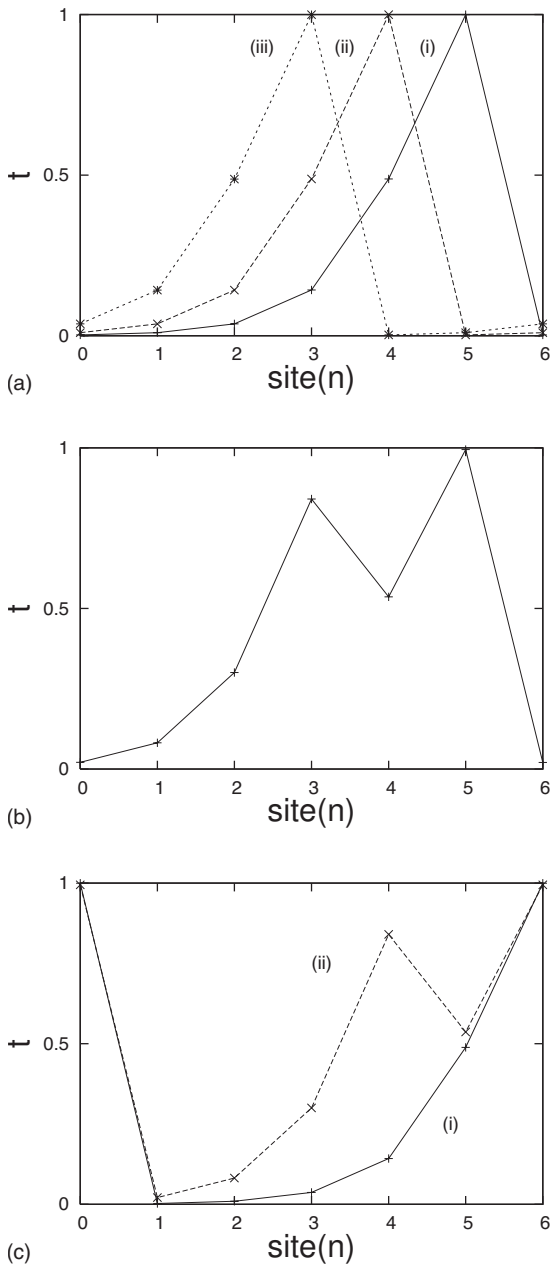

FIG. 5. Plots of t_n versus n for $n=0-6$. In (a), the curves are labeled: (i) (0.002335,4.0), (ii) (0.009315,4.0), and (iii) (0.03691,4.0). In (b), the curve is for (0.02088,4.0). In (c), the curves are labeled: (i) (0.999415,4.0) and (ii) (0.994755,4.0).

constant amplitude across the barrier and are themselves reminiscent of the Fabry–Pérot modes found in Fig. 3(a).] Nevertheless, in this oscillation, the various wave functions maintain the same form along the ridge.

The similarities between the waveguide and logistic mapping problems will be discussed in the conclusions.

IV. CONCLUSIONS

The transmission in a Kerr nonlinear barrier has been studied as a function of the parameters characterizing the barrier nonlinearity and has been compared with transmission studies made on a finite barrier described by the logistic mapping. It is found that, in the two different systems treated, general properties that arise are as follows. (1) The (t,g) plane for the Kerr barrier exhibits patternings of transmission peaks in which groupings of topographical features can be associated with Fabry–Pérot, intrinsic localized, and discrete dark solitonlike modes. The intrinsic localized and discrete dark solitonlike modes in the barrier compare well with those predicted in the infinite barrier limit. Small changes in the boundary conditions at the barrier edges can result in the shifting of modes within the barrier. Similar effects are found in the logistic mapping problem. The logistic mapping exhibits a pattern of ridges in its (t,g) plot that is reminiscent of those found in the waveguide problem. The modes in the barrier again cluster in ridges in the (t,g) transmission plot of the logistic mapping such that depending on the boundary conditions, their properties are like peak, dip, or Fabry–Pérot modes or other types of more complex modes. The logistic mapping does not support intrinsic localized modes or dark solitonlike modes, but the peak and dip modes look very similar to these and arise from similar types of boundary conditions. The boundary conditions on the logistic mapping can also be used to shift the position of the observed modes in a ridge of modes within the barrier. (2) In the waveguide problem, the intensity peaks for $0.75 \leqslant T \leqslant 1.0$ are most readily classified as in (1) and occur predominantly for $g > 0.6$. Smaller intensity peaks [see Figs. 2(a) and 2(c)–2(e)] combine features of the modes mentioned in (1) and occur for $g < 0.6$. These are modes that are significantly distorted by the boundary conditions at the barrier edges from resonances identified with modes of the infinite barrier system. For the logistic mapping, resonant transmission was defined as the unchanged transmission of the population density so that only maximally resonant modes were treated.

In a recent study, the points listed in (1) and (2) above have also been confirmed in the photonic crystal system consisting of a Kerr junction of multiple linear media photonic crystal waveguides and for a finite branching system based on the logistic mapping.[35] In the Kerr junction problem, multiple linear media photonic crystal waveguides are joined at a junction of multiple Kerr medium sites. The resonant transmission of a waveguide mode incident on the junction from one of the waveguides and transmitted into the others is plotted in the two-dimensional space of the parameters characterizing the Kerr media. Similar, topographical features to those in the waveguide barrier plot are found and the features can again be associated with intrinsic localized modes, Fabry–Pérot modes, etc. The branching problem based on the logistic mapping exhibits a similar classification of features. These are an indication of the robustness of the type of classification proposed here for finite barrier transmission problems and suggest that it is a useful classification of the properties of small nonlinear dynamical systems. The features discussed are most likely common to a large number of different types of iterative mappings and are likely to be located in general modes of nonlinear photonic crystal systems and small nonlinear systems.

An area where such classifications may be of interest is electro-optical applications. One is familiar with waveguides

and electromagnetic resonators that are used to channel or confine electromagnetic energy. Recently, there has been an interest in having electromagnetic waves interact with one another. Such interactions require nonlinear optical systems in which, through a modulation of the dielectric properties of materials by applied electric fields, one wave can interact with and control the modulation of another wave. This allows the exchange of information, and Kerr materials have been suggested as a basis for various type of switches and resonators.[19–21] For such applications, it is needed to understand the properties of the barrier and junctions of Kerr media in the parameter space of the Kerr nonlinearity in order to target the materials that can fulfill application needs. As small barriers and junctions are most easily made for applications, these are a good initial focus of such studies.

APPENDIX A

A brief summary of the origin of the difference equation formulation for the case in which the electric field of the modes is polarized parallel to the axes of the dielectric cylinders is given here. Detailed discussions are to be found in Refs. 11–13.

The photonic crystal is described by a periodic dielectric function $\epsilon(\vec{x}_\parallel)$ with $\vec{x}_\parallel$ in the plane of the Bravais lattice and perpendicular to the dielectric cylinder axes. A waveguide is introduced as a change in the dielectric constant, $\delta\epsilon(\vec{x}_\parallel)$, along a row of dielectric cylinders. The electric fields of the system are described by a Helmholtz equation that can be reformulated using standard Green's function methods into the following integral equation:

$$E(\vec{x}_\parallel) = \frac{\omega^2}{c^2}\int d^2x'_\parallel G(\vec{x}_\parallel,\vec{x'}_\parallel)\delta\epsilon(\vec{x'}_\parallel)E(\vec{x'}_\parallel), \tag{A1}$$

where $G(\vec{x}_\parallel,\vec{x'}_\parallel)$ is the Helmholtz Green's function for the photonic crystal given by $\epsilon(\vec{x}_\parallel)$.

In the case that $\delta\epsilon(\vec{x}_\parallel)$ is nonzero only in a small region about the cylinder axes of the waveguide and $E(\vec{x}_\parallel)$ changes slowly over $\delta\epsilon(\vec{x}_\parallel)$ in each such cylinder, Eq. (A1) reduces to the difference equations

$$E_{n,0} = g_p[f_{n,0}E_{n,0} + b(f_{n+1,0}E_{n+1,0} + f_{n-1,0}E_{n-1,0})] \tag{A2}$$

for a waveguide along the x axis with predominantly on-site and nearest-neighbor site interactions. In Eq. (A2), $f_{n,0}=1+\lambda|E_{n,0}|^2$ with $\lambda=0$ for linear dielectric media, $g_p = \frac{\omega^2}{c^2}\int d^2x'_\parallel G(0,\vec{x'}_\parallel)\delta\epsilon(\vec{x'}_\parallel)$ where the integral is over the cylinder centered at (0,0), and $b=\int d^2x'_\parallel G(a\hat{i},\vec{x'}_\parallel)\delta\epsilon(\vec{x'}_\parallel)/\int d^2x'_\parallel G(0,\vec{x'}_\parallel)\delta\epsilon(\vec{x'}_\parallel)$ where the integrals are made over the cylinder centered at (0,0) and a is the waveguide lattice constant. In evaluating the integrals in the definition of g_p and b, λ is always taken to be zero.

APPENDIX B

A summary of the self-consistent equations for the kink or dark solitonlike modes in an infinite Kerr barrier is given here. This was not written down explicitly in Ref. 13, but is presented here for the convenience of the reader.

The original discussions of the kink modes were made in Sec. 3.3 of Ref. 13. There, a trial wave function for a kink mode centered at (0,0) in the infinite barrier waveguide was taken to have the form

$$E_{0,0} = 0, \tag{B1}$$

$$E_{n,0} = \alpha(-1)^n(1 - A_0e^{-nq}), \tag{B2}$$

$$E_{-n,0} = -E_{n,0}. \tag{B3}$$

Upon substituting this form into the nonlinear difference equations [treating these only about (0,0) and in the $n\to\infty$ limit] gives three self-consistent equations

$$g = [1 + \lambda\alpha^2 - 2b(1 + \lambda\alpha^2)]^{-1}, \tag{B4}$$

$$(1-\Delta)\{g[1+\lambda\alpha^2(1-\Delta)^2]-1\} = gb(1-\Delta K)[1+\lambda\alpha^2(1-\Delta K)^2], \tag{B5}$$

and

$$(1-\Delta K)\{g[1+\lambda\alpha^2(1-\Delta K)^2]-1\} = gb\{(1-\Delta)[1+\lambda\alpha^2(1-\Delta)^2] + (1-\Delta K^2)[1+\lambda\alpha^2(1-\Delta K^2)^2]\} \tag{B6}$$

for g, $\Delta=A_0e^{-q}$, and $K=e^{-q}$ in terms of $\lambda\alpha^2$ and b. Approximate solutions of these were given in Ref. 13 in the limit of large fields at $n\to\infty$. In this paper, a numerical solution of Eqs. (B4)–(B6) was made.

An idea as to how an off-centered dark solitonlike mode [i.e., a mode with a wave function that is shifted from the (0,0) center lattice site] can be studied in the infinite waveguide of Kerr nonlinear media is had by taking, in place of the form given in Eqs. (B1)–(B3), the form given by

$$E_{0,0} = \alpha\delta, \tag{B7}$$

$$E_{n,0} = \alpha(-1)^n\left(1 - A_0e^{-nq} - \frac{\delta}{|\delta|}C_0|\delta|^n\right), \tag{B8}$$

$$E_{-n,0} = -\alpha(-1)^n\left(1 - B_0e^{-np} + \frac{\delta}{|\delta|}C_0|\delta|^n\right). \tag{B9}$$

Here, the new parameters A_0, B_0, q, and p become equal to those in Eqs. (B1)–(B3) in the limit $\delta=0$, and the new parameter C_0 couples to δ to produce the asymmetry of the wave function. Increasing δ from zero increases the asymmetry of the mode about (0,0).

In Table I, results are shown for $\lambda|E_{n,0}|^2$ versus $n=-2$, -1, 0, 1, and 2 for various δ in the case that $g=1.043$. (Note: For $\delta\to-\delta$, $|E_{n,0}|^2\to|E_{-n,0}|^2$.) The field intensities for $\delta=0.0$ are seen to be symmetric about $n=0$, but as δ becomes nonzero, an asymmetry appears in the system and gradually increases with increasing δ. The results were found by choosing the parameters in Eqs. (B7)–(B9) to fit equations for $E_{n,0}$ for $n=-2$, -1, 0, 1, and 2 and $n=\pm\infty$ and are valid for $|\delta|<0.04$. For large δ, more than seven parameters are needed for a good fit of the wave function over the entire waveguide.

TABLE I. Shifted dark solitonlike modes: $|E_{n,0}|^2$ versus n for various δ and g.

δ	g	$\lambda\|E_{-2,0}\|^2$	$\lambda\|E_{-1,0}\|^2$	$\lambda\|E_{0,0}\|^2$	$\lambda\|E_{1,0}\|^2$	$\lambda\|E_{2,0}\|^2$
0.2	1.043	0.13267	0.06858	0.00640	0.08860	0.10869
0.03	1.043	0.13799	0.08256	0.00014	0.08523	0.13349
0.00	1.043	0.13815	0.08470	0.00000	0.08470	0.13815

In this sense, the results for $\delta=0.2$, though giving a reasonable fit to the exact finite barrier solutions in Fig. 3(d) for $(t,g)=(4.2,1.0261)$, should be taken as only indicative of the general behavior of the system. [Note: In comparing the results in Table I with those in Fig. 3(d), the origin in n needs to be shifted by 1 and one must remember that the infinite barrier results should only approximate the field intensities observed in the finite barrier.]

*FAX: 269-387-4939; arthur.mcgurn@wmich.edu

[1] G. Nicolis and I. Prigogine, *Exploring Complexity* (Freeman, New York, 1989).
[2] S. N. Rasband, *Chaotic Dynamics of Nonlinear Systems* (Wiley, New York, 1990).
[3] T. Puu, *Attractors, Bifurcations, and Chaos* (Springer, Berlin, 2000).
[4] A. M. Turing, Philos. Trans. R. Soc. London, Ser. B **237**, 37 (1952).
[5] M. I. Rabinovich, A. B. Ezersky, and P. D. Weidman, *The Dynamics of Patterns* (World Scientific, Singapore, 2000).
[6] A. J. Koch and H. Meinhardt, Rev. Mod. Phys. **66**, 1481 (1994).
[7] S. Wolfram, *A New Kind of Science* (Wolfram Media, Urbana, 2002).
[8] A. R. McGurn and G. Birkok, Phys. Rev. B **69**, 235105 (2004).
[9] A. R. McGurn, Phys. Rev. B **65**, 075406 (2002).
[10] A. R. McGurn, Chaos **13**, 754 (2003).
[11] A. R. McGurn, Phys. Rev. B **53**, 7059 (1996).
[12] A. R. McGurn, Phys. Rev. B **61**, 13235 (2000).
[13] A. R. McGurn, Phys. Lett. A **251**, 322 (1999).
[14] M. Phihal, A. Shambrook, and A. A. Maradudin, Opt. Commun. **80**, 199 (1991).
[15] K. Sakoda, *Optical Properties of Photonic Crystals* (Springer, Berlin, 2001).
[16] J. D. Joannopoulos, P. R. Vilenueve, and S. Fan, *Photonic Crystals* (Princeton University Press, Princeton, 1995).
[17] A. R. McGurn, in *Survey of Semiconductor Physics*, edited by K. W. Boer (Wiley, New York, 2002), Chap. 33.
[18] J. D. Joannopoulos, P. R. Villeneuve, and S. Fan, Nature (London) **386**, 143 (1995).
[19] P. N. Favennec, *Photonic Crystals: Toward Nanoscale Photonic Devices* (Springer-Verlag, Berlin, 2005).
[20] A. R. McGurn, Complexity **12**, 18 (2007).
[21] A. R. McGurn, in *Nonlinear Phenomena Research Perspectives*, edited by C. W. Wang (Nova Science, New York, 2007), Chap. 8.
[22] D. L. Mills, *Nonlinear Optics* (Springer-Verlag, Berlin, 1998).
[23] R. W. Boyd, *Nonlinear Optics*, 2nd ed. (Academic, Amsterdam, 2003).
[24] P. P. Banerjee, *Nonlinear Optics* (Dekker, New York, 2004).
[25] Y. S. Kivshar and G. P. Agrawal, *Optical Solitons* (Academic, Amsterdam, 2003).
[26] A. J. Sievers and J. B. Page, in *Dynamical Properties of Solids*, edited by G. K. Horton and A. A. Maradudin (Elsevier, Amsterdam, 1995), Vol. 7, p. 137.
[27] M. Sato, B. E. Hubbard, and A. J. Sievers, Rev. Mod. Phys. **78**, 137 (2006).
[28] T. Dauxois and M. Peyrand, *Physics of Solitons* (Cambridge University Press, Cambridge, 2006).
[29] A. A. Sukhorukov and Y. S. Kivshar, J. Opt. Soc. Am. B **19**, 772 (2002).
[30] Y. S. Kivshar and B. Luther-Davies, Phys. Rep. **298**, 81 (1998).
[31] Zhang Fei, V. V. Konotop, M. Peyrard, and L. Vázquez, Phys. Rev. E **48**, 548 (1993).
[32] Y. S. Kivshar, W. Krolikowski, and O. A. Chubykalo, Phys. Rev. E **50**, 5020 (1994).
[33] J. Dziarmaga and K. Sacha, in *Advances in Soliton Research*, edited by L. V. Chen (Nova Science, New York, 2006).
[34] S. L. McCall, P. M. Platzman, R. Dalichaouch, D. Smith, and S. Schultz, Phys. Rev. Lett. **67**, 2017 (1991).
[35] A. R. McGurn, J. Phys.: Condens. Matter **20**, 025202 (2008).